A competitive algorithm for two-objective optimization : Nash game with territory splitting

Jean-Antoine Désidéri, Andrea Minelli, Enric Roca Leon

4^{th} *Inverse Problems, Design and Optimization Symposium (IPDO-2013)*
Albi, France, June 26-28, 2013

A COMPETITIVE ALGORITHM FOR TWO-OBJECTIVE OPTIMIZATION: NASH GAME WITH TERRITORY SPLITTING

Jean-Antoine Désidéri[a,b], Andrea Minelli[b,d], Enric Roca León[b,c,d]
[a] *INRIA, Centre de Sophia Antipolis Méditerranée,06902 Sophia Antipolis Cedex, France, jean-antoine.desideri@inria.fr ;*
[b] *ONERA - The French Aerospace Lab, F-92190, Meudon, France, andrea.minelli@onera.fr ;*
[c] *Eurocopter SAS, enric.roca_leon@onera.fr ;*
[d] *University of Nice - Sophia Antipolis, France.*

ABSTRACT

This contribution pertains to PDE-constrained multi-objective optimization, with a par- ticular emphasis on CPU-demanding computational applications in which the different criteria to be minimized (or reduced) originate from different physical disciplines that share the same set of design variables. A strategy has been proposed [3] for the treatment of two-discipline optimization problems in which one discipline, the primary discipline, is preponderant, or fragile. It is recommended to identify, in a first step, the optimum of this discipline alone using the whole set of design variables. Then, an orthogonal basis is constructed based on the evaluation at convergence of the Hessian matrix of the primary criterion and constraint gradients. This basis is used to split the working design space into two supplementary sub- spaces to be assigned, in a second step, to two virtual players in competition in an adapted Nash game, devised to reduce a secondary criterion while causing the least degradation to the first. The formulation is proved to potentially provide a set of Nash equilibrium solutions originating from the original single-discipline optimum point by smooth continuation, thus introducing competition gradually. This approach is first demonstrated over a test-case of aero-structural aircraft wing shape optimization, in which the eigen-split-based optimization reveals clearly superior [2] [4]. A significant reduction of 8 % of the structural criterion was realized while maintaining the flowfield configuration close to optimality (drag increase ¡ 3 %), by an automatic procedure of orthogonal decomposition of the parameter space (see Figure 1). Other examples of optimum-shape design in compressible aerodynamics will be provided. The first example relates to the aerodynamic shape optimization of a supersonic business jet, in which the primary criterion is again wave drag under a lift constraint, whereas the secondary criterion is a measure of the sonic boom intensity for a supersonic business jet, and both criteria ought to be minimized. The second example is a two-point shape optimization of a helicopter rotor blade in which the primary criterion is the Figure of Merit in hover condition (to be maximized), whereas the secondary criterion is the power to be developed to maintain forward motion (to be minimized)

1 INTRODUCTION

In engineering design, optimization may proceed hierarchically by several steps of refinement. The first step involves the minimization of a preponderant primary objective function in natural relation with the basic functionality of the system. For example, optimum-shape design in aerodynamics for a transport aircraft usually begins with a drag minimization subject to a lift constraint, because this conditions the fundamental mission of the transport vehicle (range, kerosene consumption, environmental impact); in a second step, one is concerned with the optimization of aerodynamic moments (stability, maneuverability); then other disciplines are introduced, structural design (mass, stiffness) in particular. Hence, the designer faces the dilemma of proposing a solution close to the optimum of the preponderant discipline alone, still incorporating multi-objective concepts. This difficult problematics is particularly acute when the preponderant discipline is compressible aerodynamics, since the functionals, usually aerodynamic coefficients, are then computed from mathematically weak solutions, that is, flow-fields in the presence of shocks, and possibly other types of singularities. Notably, aircraft-wing drag-minimization often results in a delicate design of the geometry in the shock region, thus making the flow-field solution, and the corresponding design solution very fragile. Additionally, the problem is well-known to be subject to multi-modality by the evidence of a large number of local minima.

In such a situation of fragile preponderant discipline, it is very difficult to alter even slightly the single-discipline optimum design without disrupting dramatically the main performance. Our algorithm has been devised precisely to handle such situations. Here, we summarize our method and main theoretical results, and refer to [**?**][**?**][14] for a detailed analysis, and proceed with two design examples pertaining to compressible aerodynamics.

2 TWO-DISCIPLINE OPTIMIZATION BY TERRITORY SPLITTING AND NASH GAME

We consider the case of two disciplines, A (primary) and B (secondary), associated with the objective-functions $J_A(\mathbf{x})$ and $J_B(\mathbf{x})$, functions of the same finite-dimensional design vector $\mathbf{x} \in \mathbb{R}^N$. The primary objective-function $J_A(\mathbf{x})$ is explicitly subject to K equality constraints $g(\mathbf{x}) = 0$ ($g : \mathbb{R}^N \to \mathbb{R}^K$). We also assume that possible additional constraints on the secondary objective-function $J_B(\mathbf{x})$ are formally incorporated in its definition by projections.

Basically, we proceed in three steps:

1. Step 1: Use an appropriate optimizer to calculate the solution $\mathbf{x}_A^\star$ in the whole design search space (e.g. $\mathbb{R}^N$) of the primary objective-function minimization subject to the equality constraints :

$$\mathbf{x}_A^\star = \mathsf{Argmin}\, J_A(\mathbf{x}) \quad \text{subject to : } g(\mathbf{x}) = 0 \quad (\mathbf{x} \in \mathbb{R}^N) \tag{1}$$

   (Note that optimality of J_A under constraints requires that $\nabla J_A^\star + \sum_{k=1}^K \lambda_k \nabla g_k^\star = 0$, where the gradient $\nabla J_A^\star = \nabla J_A(\mathbf{x}_A^\star)$, the constraint-gradients $\nabla g_k^\star = \nabla g_k(\mathbf{x}_A^\star)$, and the Lagrange multipliers $\lambda_k \geq 0, \forall k = 1, \ldots, K$.)

2. Step 2: Identity the Hessian matrix $H_A^\star = \nabla^2 J_A(\mathbf{x}_A^\star)$. Apply the Gram-Schmidt process to the constraint-gradients and get first K orthogonal vectors $\{\omega^1, \omega^2, \ldots, \omega^K\}$ assumed to be linearly independent (standard "constraint qualification" condition). Form the projection matrix $P = I_N - \sum_{k=1}^K \left[\omega^k\right]\left[\omega^k\right]^t$, define the reduced Hessian matrix $H'_A = PH_A^\star P$ and proceed with its diagonalization $H'_A = \Omega \mathcal{H}' \Omega^t$.

   (The eigen-modes, column vectors of matrix H'_A are arranged in a special order: the first K are precisely chosen to be $\{\omega^1, \omega^2, \ldots, \omega^K\}$, and the remaining ones are arranged in decreasing order of the corresponding positive eigenvalue of H'_A. In this way, the span of the first K eigen-modes contains the steepest-descent direction of the primary objective function, namely ∇J_A^*; inversely, the tail eigen-modes, hierarchically arranged according to the associated Rayleigh quotient, are associated with directions of least influence on $J_A(\mathbf{x})$.)

3. Step 3: Consider the splitting of parameters defined by :

$$\mathbf{x} = \mathbf{x}(\mathbf{u}, \mathbf{v}) = \mathbf{x}_A^* + \Omega \begin{pmatrix} \mathbf{u} \\ \mathbf{v} \end{pmatrix}, \quad \mathbf{u} = \begin{pmatrix} u_1 \\ \vdots \\ u_{N-p} \end{pmatrix} \in \mathbb{R}^{N-p}, \quad \mathbf{v} = \begin{pmatrix} v_p \\ \vdots \\ v_1 \end{pmatrix} \in \mathbb{R}^p \ (1 \leq p \leq N-K). \tag{2}$$

   Let ϵ be a small positive parameter ($0 \leq \epsilon \leq 1$), and let $\overline{\mathbf{x}}_\epsilon$ denote the Nash equilibrium point associated with the concurrent optimization problem :

$$\begin{cases} \min\limits_{\mathbf{u} \in \mathbb{R}^{N-p}} J_A \\ \text{Subject to : } g = 0 \end{cases} \quad \text{and} \quad \begin{cases} \min\limits_{\mathbf{v} \in \mathbb{R}^p} J_{AB} \\ \text{Subject to : no constraints} \end{cases} \tag{3}$$

   where

$$J_{AB} := \frac{J_A}{J_A^*} + \epsilon \left(\theta \frac{J_B}{J_B^*} - \frac{J_A}{J_A^*} \right) \tag{4}$$

   and θ is a strictly-positive relaxation parameter ($\theta < 1$: under-relaxation; $\theta > 1$: over-relaxation).

Then (see [**?**] or [14] for proofs and details) :

- The orthogonal split is optimal in the sense of reverse principal direction decomposition.
- The Nash-game formulation is consistent with the single-discipline optimization, in the following sense: For $\epsilon = 0$, the Nash-equilibrium exists and it is equal to the single-discipline optimum $\mathbf{x}_A^\star$:

$$\overline{\mathbf{x}}_0 = \mathbf{x}_A^* \tag{5}$$

  This is our main theoretical result and it is equivalent to making the following two statements concerning (3) for $\epsilon = 0$: *(i)* the (constrained) sub-problem on J_A admits the solution $\overline{\mathbf{u}} = 0$ (in $\mathbb{R}^{N-p}$) if $\mathbf{v}$ is set fixed equal to 0 (in $\mathbb{R}^p$); symmetrically, *(ii)* the (unconstrained) sub-problem on J_{AB} ($= J_A/J_A^\star$ for $\epsilon = 0$) admits the solution $\overline{\mathbf{v}} = 0$ (in $\mathbb{R}^p$) if $\mathbf{u}$ is set fixed equal to 0 (in $\mathbb{R}^{N-p}$).

In the above, statement *(i)* is evident because although the search is made in a sub-space of reduced dimension, if $\mathbf{v} = 0$, setting $\mathbf{u} = 0$ gives $\mathbf{x} = \mathbf{x}_A^\star$ which yields the global optimum of the constrained problem on the primary objective-function J_A. However, statement *(ii)* is non-trivial and essential; it holds since, for $k \leq p$:

$$\frac{\partial J_{AB}}{\partial v_k} = \frac{1}{J_A^\star}\frac{\partial J_A}{\partial v_k} = \frac{1}{J_A^\star}\nabla J_A^\star \cdot \frac{\partial \mathbf{x}}{\partial v_k} = \frac{1}{J_A^\star}\nabla J_A^\star \cdot \omega^{N-k+1} = 0 \tag{6}$$

where the scalar product is equal to 0 since, by construction, $\nabla J_A^\star \in \mathsf{Sp}\left(\omega^1, \omega^2, \ldots, \omega^K\right)$, and the splitting matrix Ω is orthogonal. $\square$

Consequently, as ϵ varies a continuum of Nash equilibriums is generated parameterized by ϵ

$$\overline{\mathbf{x}}_\epsilon = \mathbf{x}(\overline{\mathbf{u}}_\epsilon, \overline{\mathbf{v}}_\epsilon) \tag{7}$$

originating from the point of optimality $\mathbf{x}_A^\star$ of discipline A alone.

- The efficiency, in terms of the primary objective function J_A, is robust w.r.t. small variations in ϵ.
  Letting $j_A(\epsilon) = J_A\left(\overline{\mathbf{x}}_\epsilon\right)$ and $j_{AB}(\epsilon) = J_{AB}\left(\overline{\mathbf{x}}_\epsilon\right)$ implies that $j'_A(0) = 0$ and $j'_{AB}(0) = \theta - 1 \leq 0$, and consequently:
  $$j_A(\epsilon) = J_A^* + O(\epsilon^2) \qquad j_{AB}(\epsilon) = 1 + (\theta - 1)\,\epsilon + O(\epsilon^2) \tag{8}$$
  Hence, with under-relaxation ($\theta < 1$), the auxiliary function J_{AB} initially diminish as ϵ increases. However, in practical experiments, one usually set θ to 1.

- Case of linear equality constraints. In this case, the continuum of Nash equilibriums is parameterized as follows:
  $$u_k(\epsilon) = 0 \quad (1 \leq k \leq K) \qquad \overline{\mathbf{x}}_\epsilon = \mathbf{x}_A^* + \sum_{k=K+1}^{N-p} u_k(\epsilon)\,\omega^k + \sum_{j=1}^{p} v_j(\epsilon)\,\omega^{N+1-j} \tag{9}$$

- Special case: $K = 1$ and $p = N - 1$. Then, the Nash equilibrium point $\overline{\mathbf{x}}_\epsilon$ *is Pareto optimal*.

These theoretical results provide a framework to formulate a continuation procedure yielding a continuum of Nash equilibriums realising gains in a secondary discipline in the smooth continuity of a primary-discipline optimum point. Demonstration of this approach in the context of the aero-structural wing-shape optimization of a business jet has been provided in [**?**][**?**][14].

We close this section with remarks of computational nature.

Firstly, in above Steps 1 and 2, if first or second derivatives are not available, formally or by finite-differences, they may be approximated, in practice, via meta-models.

Secondly, Step 3 involves two embedded loops. The outer loop corresponds to the incrementation of the continuation parameter ϵ to achieve a continuum of Nash equilibriums. In the inner loop, for a given ϵ, the design parameters evolve towards equilibrium after successive iterations of exchange of sub-vectors; between two exchanges, each sub-vector is upgrading by a few minimization steps to reduce either J_A or J_{AB} conducted in either supplementary sub-space. These two optimization steps are independent, and can be performed in parallel, using possibly-different optimization methods (e.g. one stochastic, and the other deterministic) and operating on different physics, thus different codes.

Thirdly, in the next two sections, two applications are presented, in which indeed, after the single-discipline optimization of Step 1 has been conducted with the support of a high-fidelity CFD code, surrogate models for J_A, J_B and g have been constructed from a database of new high-fidelity simulations about $\mathbf{x} = \mathbf{x}_A^\star$; then, in Step 3, the two parallel optimizations have been conducted on the surrogate models themselves, and at each achieved equilibrium point, the corresponding design has been re-evaluated by the high-fidelity codes, outside of the Nash-game coordination inner loop.

Fourthly, in treating complex nonlinear physics, if meta-models are used in the optimization algorithm, it may be useful to upgrade these surrogate models at least once in the course of the optimization process.

3 AERO-ACOUSTIC SHAPE OPTIMIZATION OF A WING-BODY SUPERSONIC CONFIGURATION

In the case of the development of a supersonic business jet, aerodynamics and acoustics represent the two antagonists *par excellence* [17]. A body flying at supersonic speed, contrary to subsonic aircraft, raises the problem of sonic boom in addition to aerodynamic performance [21]. The aero-acoustic multi-objective problem can be stated as follows:

$$\text{Minimize} \begin{cases} J_A(\mathbf{x}) = c_D & \text{subject to :} \quad g = c_L - c_{L_0} \geq 0 \quad \text{with } c_{L_0} = 0.1 \\ J_B(\mathbf{x}) = \sum \Delta p & \text{subject to :} \quad \text{no constraints} \end{cases} \tag{10}$$

where c_D is the drag coefficient, c_L the lift coefficient and $\sum \Delta p$ is the sum of the shock overpressures in the under-track ground signature.

In this work, following [29], the aerodynamic performance evaluation is performed using the Onera elsA CFD code [2]. Invisicid Euler equations with Roe flux [8], Harten entropy correction [24] and the Van Albada flux limiter[9] are used to describe the flow in the near-field. Structured CFD grids on the half configuration were used in the calculations. The domain is a half cylinder with a conical cap and base made of 6,030,298 nodes. It extends from the configuration up to 4 body lengths. The pressure field is directly extracted over a cylinder that surrounds the configuration and the signal is propagated to the ground using the ray-tracing code TRAPS [25].

The normalized design variables (components of $\mathbf{x}$) are: nose deflection (x_1), nose-section radius (x_2), cabin-section radius (x_3), relative wing position along fuselage (x_4), and dihedral angle (x_5). Nash games iterations are performed on a surrogate model and the equilibrium points are evaluated at the equilibrium point by the high-fidelity CFD-based model. A first Kriging model for each discipline and for the constraint is created using a LHS database made up of 45 individuals.

To identify the continuum of Nash equilibrium solutions, the following steps are performed:

- The minimization of the drag coefficient with constraint on lift $g : c_l - 0.1 \geq 0$ is obtained using the algorithm CMA-ES[26]. After some 1200 iterations the optimum is found at $J_A^* = 81.458$ Pa with $g = 0.002$. The corresponding design vector is $\mathbf{x} = [-0.558, -0.836, -0.506, -0.434, -1]$;
- The reduced Hessian is calculated and diagonalized yielding the following orthogonal splitting matrix:

$$\Omega = \begin{bmatrix} -0.1967 & -0.1839 & 0.0944 & -0.8251 & -0.4876 \\ -0.1257 & -0.4079 & -0.9042 & 0.0107 & 0.0114 \\ -0.6606 & -0.5744 & 0.3548 & 0.3282 & -0.0037 \\ -0.7055 & 0.6776 & -0.2077 & -0.0095 & 0.0049 \\ 0.1070 & 0.1036 & -0.0672 & 0.4596 & -0.8730 \end{bmatrix};$$

  Then, a 2+3 split is adopted, in which 2 variables are assigned to aerodynamics and 3 to acoustics. In this way, the strategy of player B is in the span of the three eigenmodes of least influence on the primary discipline A.
- A continuation process is developed by incrementing the parameter ϵ by step of 0.05. For each value of ϵ, optimization iterations are performed potentially in parallel by SQP [27] for J_A, and by the Nelder-Mead simplex algorithm for J_{AB}, sub-vectors are exchanged, and this repeats until convergence to the Nash equilibrium solution.

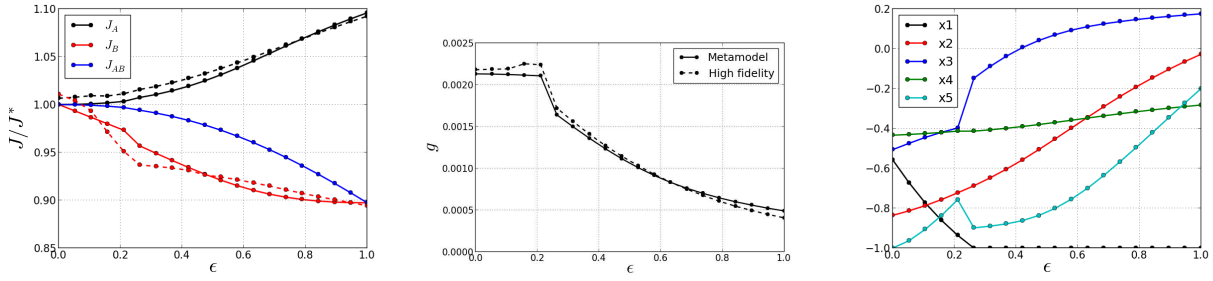

(a) Continuum of the Nash equilibrium (b) Constraints function (c) Variables

Figure 1: Continuum of the Nash equilibrium solutions. Continuous lines represent evaluations using surrogate models, while dotted lines represent evaluations using high-fidelity models.

Figure 1(a) shows the history of the continuum of the Nash equilibria. For $\epsilon = 0$ all the three curves initiate at the value 1. J_A and J_{AB} have zero slope due to the problem formulation which is consistent with the original optimum. As ϵ increases drag degrades monotonically, while J_{AB}, and J_B by consequence diminish. During the first iterations, the nose is deflected downward (x_1) (see figure 1(c)). At ϵ close to 0.25, x_1 reaches its low-bound constraint. A new equilibrium point is found at the next iteration increasing the cabin radius (x_3) and keeping the wing closer to the nose (x_5). This new configuration causes an abrupt decay of g and J_B. The constraints function g is satisfied all along the iterations (see figure 1(b)), but the margin on the constraints reduces away from the aerodynamic optimum $\mathbf{x}_A^*$. The low drag configuration has a dihedral angle (x_5) equal to zero while as shown in Fig. 2(c) for values of $\epsilon \geq 0.5$ the angle is almost equal to 3^o.

The equilibrium points evaluated using the Kriging model are re-evaluated using the high fidelity models. The new curves in dotted lines in figures (1(a)) and (1(b)) are in agreement with the results obtained using the low-fidelity model.

The accurate definition of the Kriging model has permitted to obtain the high correlation between low and high fidelity model. From a design point of view solutions at point $\epsilon = 0.25$ is the most interesting. In fact considering the high-fidelity prediction drag is degraded by only 1%, while the acoustic function is reduced by more than 7%.

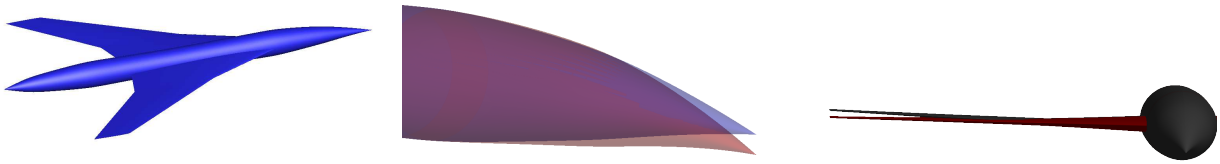

(a) Initial low-drag configuration (b) Nose deflection from $\epsilon = 0$ to $\epsilon = 0.5$ (c) Dihedral angle increases from $\epsilon = 0.5$ to $\epsilon = 1$

Figure 2: Main geometry modification during Nash game convergence. In blue the initial low-drag configuration ($\epsilon = 0$), in red the configuration at $\epsilon = 0.5$, in black the configuration at $\epsilon = 1$

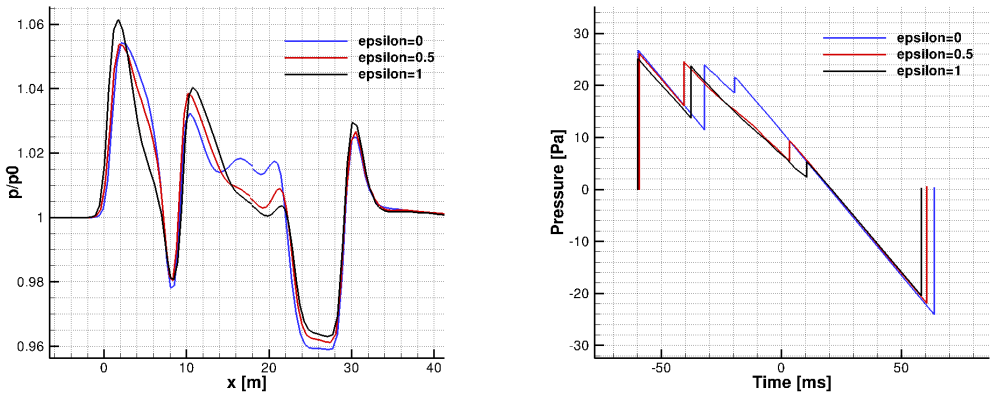

(a) Pressure signature ($p/p0$) extracted under-track at z=h_Z-10m (b) Under-track ground signature

Figure 3: Near-field and ground pressure signal for different along the Nash equilibrium continuum.

Three configurations are retained for comparative analysis at different ϵ equal to 0, 0.5 and 1. As ϵ increases, the nose shock is bounded in a region close to the nose top. The consequence is an increased nose shock amplitude, but more localized. The area under the first peak of the near field pressure signature is reduced as ϵ tends to 1. This signature is directly related to the Whitham F-function [28], and in particular the first peak area is related to the nose shock amplitude and position. A reduced area determines a reduced front shock for the ground signature (Fig. 3(b)).

The shock related to the wing leading edge is progressively increased as ϵ tends to 1. The consequence is a reduction of the pressure expansion after the first peak of the ground signature as already seen in the analysis of the Pareto front obtained using the cooperative strategy [**?**]. The low-pressure region at the trailing edge of the wing and at the corresponding junction with the fuselage is increased. The interaction with the bow shock pattern determines at ground level a reduced amplitude of the rear shock. All the shocks in the ground signature contribute to the reduction of J_B. Nose shock overpressure is reduced by 2 Pa as well as the wing shock, while the bow shock shows a reduction by more than 4% from $\epsilon = 0$ to $\epsilon = 1$.

4 AERODYNAMIC SHAPE OPTIMIZATION OF HELICOPTER ROTOR BLADES

The aerodynamic optimization of helicopter rotor blades typically requires to find a compromise between the optimal design in the stationary hover conditions, and forward-flight optimal configurations, and these concepts are strongly

antagonistic. The described methodology [30] is demonstrated on the model rotor ERATO [1], which presents a complex planform geometry including forward and backward sweep. The primary criterion is the maximization of the Figure of Merit (FM), which is a measure of the rotor efficiency (defined as the ratio between the ideal and the actual power required to hover). The secondary criterion is the minimization of the required rotor power in forward flight (P). An implicit constraint is added in the deformation process in order to assure constant thrust-weighted solidity (i.e. the ratio between total blade area and disk area weighted by the sectional thrust force) as recommended in the literature [10, 3]. Finally, an additional constraint is imposed on the maximum admissible value of static link loads (L), related to the torque value at the blade root in forward flight. The problem is formulated as follows:

$$\text{Minimize} \begin{cases} J_A(\mathbf{x}) = 100 * (1 - FM) \\ J_B(\mathbf{x}) = P \end{cases} \qquad \text{subject to :} \quad g = L - L_0 \geq 0 \tag{11}$$

The hover performance computations are conducted employing elsA [2], developed at ONERA. The Reynolds-Averaged Navier-Stokes (RANS) equations are used, employing the Kok $k - \omega$ turbulence model [6] with a shear stress transport (SST) correction [7]. The flux is discretized using a 2nd order Roe's scheme [8] along with Van Albada limiter [9]. The time integration is performed using an implicit algorithm based on a backward Euler scheme. The mesh strategy is the same for all hover simulations: a quarter of rotor mono-block mesh of 0.81 million points with a C-H grid topology (Fig. 4). In forward flight, Eurocopter's HOST code [4] is used to evaluate the performance, taking into account blade deformations with a 1D Euler-Bernoulli beam model coupled with a simplified aerodynamics model based on lifting-line theory. The chosen design point for the ERATO rotor in advancing flight is at $V = 260\ km/h$, $Z_b = 12.5$ (thrust coefficient) and drag $C_x \times S = 0.1$ (S: dimensionless reference surface) for a tip Mach number $M_{tip} = 0.617$. The blade is parametrized using 2 Bézier laws and 1 cubic spline of five control points each piloting twist, chord and sweep distributions respectively. Finally, the collective pitch is added as variable, for a total of 16 design parameters. The procedure presented by Dumont [3] involving the use of the discrete adjoint is employed to conduct a single objective optimization of the primary criterion. Convergence is attained after 31 CFD iterations plus 8 adjoint evaluations, employing the descent algorithm CONMIN [5], requiring a total computational time of 33 CPU hours. The obtained hover optimum increases the initial value of maximal FM by approximately 7.8%, presenting better flight capabilities at high rotor thrust, even if the consumed power is significantly increased.

Subsequently, a Nash Game optimizing twist, chord and sweep laws in forward flight is conducted, employing a Kriging metamodel for the primary discipline. The metamodel is initialized using 150 samples obtained via Latin Hypercube Sampling [11]. Estimates of the metamodel error are computed using K-fold stratified cross-validation techniques, as recommended by Kohavi [12] using the K-means stratification strategy proposed by Diamantidis [13]. The metamodel was iteratively updated with the maximum expected improvement point as well as the computed global minimum while monitoring the global bias, defined as the root mean square deviation. The iterative updating process of the metamodel was stopped after 22 additional points were added to the initial database, when no further improvements were obtained for 3 consecutive iterations. The split matrix is thus obtained using the Hessian (computed via the metamodel). In this case, 8 variables are assigned to each player (8+8 split). The CONMIN algorithm is used for both players at each Nash iteration: in hover (metamodel) single optimizations are performed until convergence, while in forward flight the optimization is limited to 2 gradient iterations. The maximum number of information exchanges between players is limited to 2. Finally, the continuation parameter ϵ is incremented by step of 0.1.

The results of the Nash Game are shown in Fig. 5. The curves are normalized with respect to the values at the initial hover optimum J_i*. The dashed lines (J_{i0}/J_i*) mark the baseline rotor performance, the upper line representing the initial Figure of Merit value (with respect to the hover optimum). Gains on hover performance are thus represented by values bellow this line. The lower dashed line represents the ERATO consumed power, with points signifying an increase in consumption being situated above the line. The Nash equilibria obtained using the surrogate model were subsequently reevaluated using high-fidelity CFD. A good agreement near the initial hover optimum is found (up to $\epsilon = 0.7$). The surrogate model performance is significantly degraded as the Nash Game advances and the optimization algorithm searches further in regions near the limit of validity of the metamodel. An important error in the computation of the equilibrium by the metamodel is obtained at $\epsilon = 0.8$ and remains considerable up to $\epsilon = 1$. However, and most importantly, the metamodel trends are generally similar to the ones shown by the high-fidelity code.

In this case, the designer may consider that the equilibrium at $\epsilon = 0.7$ offers the best compromise solution. However, for illustration purposes, the resulting blades at $\epsilon = 0$ and $\epsilon = 1$ are presented in Fig. 7.

Some indicators of performance in forward flight are presented in Fig. 6. The figures represent the rotor disk, showing the total power and sectional lift of the blade for a complete revolution (which shows asymmetric values in forward flight). The values are given as deltas with respect to the baseline rotor. The left column corresponds to the optimum in hover ($\epsilon = 0$), while the right column corresponds to the rotor at $\epsilon = 1$. The power increase at the fore blade zone shown by the hover optimum ($\epsilon = 0$) is balanced for the Nash equilibrium, which reproduces the power distribution of the ERATO blade with a slight increase at $\psi = 360°$. In addition, the twist reduction at the tip combined with the chord reduction

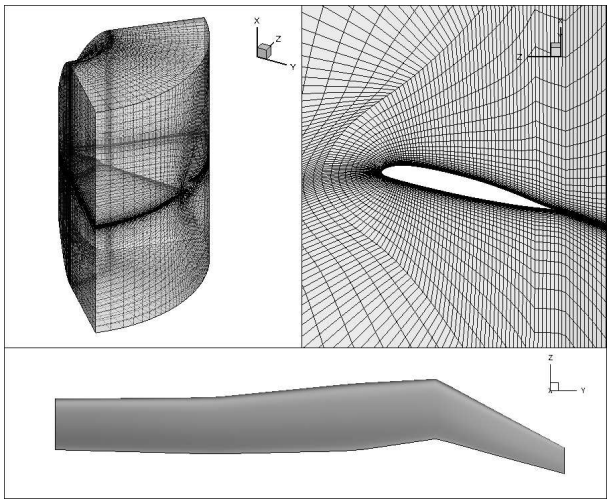

Figure 4: Mesh strategy and blade geometry.

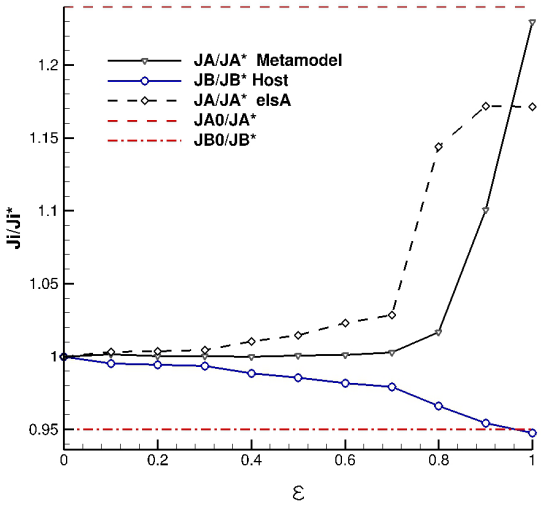

Figure 5: Continuum of the Nash equilibrium.

in the same zone leads to an overall gain in lift in the advancing side, as shown in the sectional lift figure. The last equilibrium ($\epsilon = 1$) obtains a 1% power reduction with respect to the baseline (-5.5% w.r.t. $\epsilon = 0$) while conserving a gain of approximately 2.6% in the Figure of Merit.

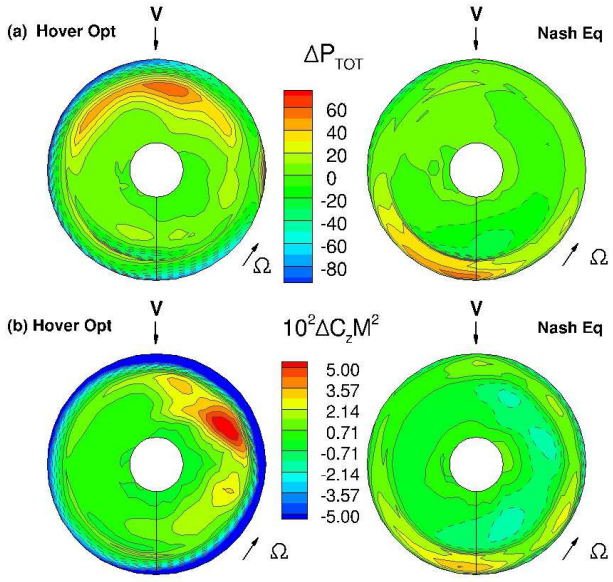

Figure 6: Total power (a) and sectional lift (b) variations in forward flight of the hover optimum and the Nash compromise at $\epsilon = 1$ with respect to ERATO (game including twist, chord and sweep).

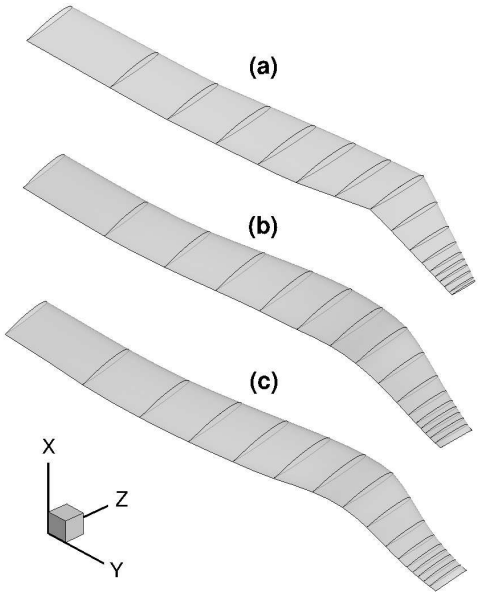

Figure 7: Blade comparison: (a) ERATO baseline, (b) hover optimum ($\epsilon = 0$) and (c) last Nash equilibrium ($\epsilon = 1$).

5 CONCLUSIONS

Nash games offer a versatile formulation to achieve trade-offs in concurrent engineering when two or more objective-functions originating from different disciplines are antagonistic in the design process. In stringent optimization situations, after a preponderant or fragile discipline has been optimized, it is very difficult to improve any other criterion. We have shown how to elaborate a territory splitting, that is a split of the design variables, permitting then to achieve this goal at a minimal cost in terns of degradation of the primary discipline. The technique is based on approximating the Hessian

matrix and constraint gradients, and to identify an orthogonal basis of principal directions, and to formulate the Nash game in this basis, after appropriate ordering of the eingen-modes.

We have shown the efficiency of this method in two complex optimum-shape design problems in which the primary discipline is the drag minimization of a flying vehicle in steady conditions: the aero-acoustic wing-shape optimization of a supersonic business jet (SSBJ), and a two-point helicopter rotor-blade optimization. In both cases, the secondary objective-function is improved while drag is only increased a few percents from the absolute minimum.

References

[1] J.Prieur and W.R. Splettstoesser, "Erato - an onera-dlr cooperative programme on aeroacoustic rotor optimization," in *25th European Rotorcraft Forum*, September 1999. Rome, Italy.

[2] L.Cambier and J.Veuillot, "Status of the elsa cfd software for flow simulation and multidisciplinary applications," in *46th AIAA Aerospace Science Meeting and Exhibit*, vol.664, 2008.

[3] A.Dumont, A.LePape, J.Peter, and S.Huberson, "Aerodynamic shape optimization of hovering rotors using a discrete adjoint of the reynolds-averaged navierstokes equations," *Journal of the American Helicopter Society*, vol.56, no.3, pp.1–11, 2011.

[4] B.Benoit, A.Dequin, K.Kampa, W.VonGranhagen, P.Basset, and B.Gimonet, "Host, a general helicopter simulation tool for germany and france," in *American Helicopter Society 56th Annual Forum*, May 2000. Virginia Beach, USA.

[5] G.N. Vanderplaats, "Conmin: A fortran program for constrained function minimization," tech. rep., NASA, August 1973. NASA-TM-X-62282.

[6] J.C. Kok, "Resolving the dependence on freestream values for the k-omega turbulence model," *AIAA journal*, vol.38, no.7, pp.1292–1295, 2000.

[7] F.Menter, "Two-equation eddy-viscosity turbulence models for engineering applications," *AIAA Journal*, vol.32, no.8, pp.1598–1605, 1994.

[8] P.L. Roe, "Approximate riemann solvers, parameter vectors, and difference schemes," *Journal of computational physics*, vol.43, no.2, pp.357–372, 1981.

[9] G.VanAlbada, B.VanLeer, and W.RobertsJr, "A comparative study of computational methods in cosmic gas dynamics," *Astronomy and Astrophysics*, vol.108, pp.76–84, 1982.

[10] G.J. Bingham, "The aerodynamic influences of rotor blade taper, twist, airfoils and solidity on hover and forward flight performance.," tech. rep., DTIC Document, 1982.

[11] M.D. McKay, R.J. Beckman, and W.J. Conover, "Comparison of three methods for selecting values of input variables in the analysis of output from a computer code," *Technometrics*, vol.21, no.2, pp.239–245, 1979.

[12] R.Kohavi, "A study of cross-validation and bootstrap for accuracy estimation and model selection," in *International joint Conference on artificial intelligence*, vol.14, Lawrence Erlbaum Associates Ltd, 1995.

[13] N.Diamantidis, D.Karlis, and E.Giakoumakis, "Unsupervised stratification of cross-validation for accuracy estimation," *Artificial Intelligence*, vol.116, no.1, pp.1–16, 2000.

[14] Désidéri, J.A., "Cooperation and competition in multidisciplinary optimization - Application to the aero-structural aircraft wing shape optimization", *Computational Optimization and Application*, **52** (2012), pp. 3-28, Springer Netherlands.

[15] Desideri, J.A., "Multiple-Gradient Descent Algorithm (MGDA)". *INRIA RR 6953, 2009.* 2009.

[16] J. F. Nash, "Non-cooperative games", *Ann. Math., vol. 54, pp. 286-295, 1951.*

[17] C. M. Darden. "Limitations of linear theory for sonic boom calculations," *Journal of Aircraft, Vol. 30, No. 3 (1993), pp. 309-314.*

[18] Désidéri, J.A., "Split of Territories", *INRIA RR 6108, 2007.*

[19] Powell M.J.D. , "A direct search optimization method that models the objective and constraint functions by linear interpolation", *in Advances in Optimization and Numerical Analysis, eds. S. Gomez and J-P Hennart, Kluwer Academic (Dordrecht), pp. 51-67,1994.*

[20] J.A. Nelder and R. Mead, "A simplex method for function minimization". *Comput. J. 7 (1965) 308.*

[21] Plotkin, K.J., "State of the Art of Sonic Boom Modeling," *The Jo. of the Acoustical Society of America*, Vol. III, No. 1, pp. 530-536, 2002.

[22] Cambier, L. and Gazaix M. 2002. "An Efficient Object-Oriented Solution to CFD Complexity." *AIAA 02-0108*

[23] T.T. Bui, CFD Analysis of Nozzle Jet Plume Effects on Sonic Boom Signature. *NASA TM-2009-214650*, 2009

[24] A. Harten, J. M. Hyman and P. D. Lax, On finite-difference approximations and entropy conditions for shocks, Comm. Pure Appl. Math., 29 (1976), pp. 297-322.

[25] Taylor, A.D. 1980. "The TRAPS Sonic Boom Program." *NOAA Technical memorandum ERL-ARL-87*

[26] Hansen, N., Ostermeier, A., 2001. "Completely derandomized self-adaptation in evolution strategies." *Evolutionary Computation, 9(2) pp. 159-195.*

[27] Gill, P.E., Murray, W., and Wright, M.H. 1986. "Practical Optimization", Academic Press, London ISBN 0-12-283952-8.

[28] Whitham, G.B., "The Flow Pattern of a Supersonic Projectile," *Communications on pure and applied mathematics, Vol. 5, No.3, pp 301-348, 1952.*

[29] Minelli, A., Salah el Din, I., carrier, G., Zerbinati, A., and Désidéri, J.-A., "Cooperation and Competition Strategies in Multi-objective Shape Optimization Application to Low-boom/Low-drag Supersonic Business Jet", *AIAA Applied Aerodynamics Conference 2013, 24-27TH June, San Diego CA.*

[30] Roca Léon, E., Le Pape, A., Désidéri, J.-A., Alfano, D., and Costes, M., "Concurrent Aerodynamic Optimization of Rotor Blades Using a Nash Game Method", *AHS 69th Annual Forum, Phoenix, Arizona, May 21-23, 2013.*